

Provided for non-commercial research and education use.
Not for reproduction, distribution or commercial use.



(This is a sample cover image for this issue. The actual cover is not yet available at this time.)

This article appeared in a journal published by Elsevier. The attached copy is furnished to the author for internal non-commercial research and education use, including for instruction at the authors institution and sharing with colleagues.

Other uses, including reproduction and distribution, or selling or licensing copies, or posting to personal, institutional or third party websites are prohibited.

In most cases authors are permitted to post their version of the article (e.g. in Word or Tex form) to their personal website or institutional repository. Authors requiring further information regarding Elsevier's archiving and manuscript policies are encouraged to visit:

<http://www.elsevier.com/copyright>



Contents lists available at SciVerse ScienceDirect

Earth and Planetary Science Letters

journal homepage: www.elsevier.com/locate/epsl

Comparative zircon U–Pb geochronology of impact melt breccias from Apollo 12 and lunar meteorite SaU 169, and implications for the age of the Imbrium impact

Dunyi Liu^a, Bradley L. Jolliff^{b,*}, Ryan A. Zeigler^{b,c}, Randy L. Korotev^b, Yushan Wan^a, Hangqiang Xie^a, Yuhai Zhang^a, Chunyan Dong^a, Wei Wang^a

^a Beijing SHRIMP Center, Institute of Geology, Chinese Academy of Geological Sciences, China

^b Department of Earth and Planetary Sciences and the McDonnell Center for the Space Sciences, Washington University in St. Louis, One Brookings Drive, St. Louis, MO 63130, United States

^c ARES – Acquisition & Curation, NASA, Lyndon B. Johnson Space Center, Mail Code KT, 2101 NASA Parkway, Houston, TX 77058, United States

ARTICLE INFO

Article history:

Received 29 July 2011

Received in revised form 8 December 2011

Accepted 9 December 2011

Available online xxxx

Editor: R.W. Carlson

Keywords:

SHRIMP U–Pb analysis

impact-melt breccia

Apollo 12

SaU 169

Imbrium

Moon

ABSTRACT

The ages of zircons from high-Th impact-melt breccias (IMBs) from meteorite Sayh al Uhaymir (SaU) 169 and from rock fragments in soil samples from Apollo 12 have been determined using the SHRIMP-II ion microprobe. The IMBs are very similar to each other in chemistry, mineralogy and texture, and the zircons from the KREEP-rich (high-Th) crystalline impact melt have similar U and Th contents and identical ages, within uncertainties, of 3920 ± 13 (2σ) Ma (SaU 169) and 3914 ± 7 (2σ) Ma (Apollo 12). The age results support the idea that the high-Th IMBs (Apollo 12 and SaU 169) formed in the same impact event. The similarity of composition and age suggest that SaU 169 and the high-Th IMB fragments of Apollo 12 originated from the same area of the Procellarum KREEP Terrane. We interpret the age of zircon grains in the Apollo 12 high-Th IMB as a precise and direct determination of the age of the Imbrium impact. This age is significantly older than the commonly cited age of 3.85 Ga but is similar to recent determinations from SIMS U–Pb dating of Apollo 14 apatite grains and with anticipated revision of ages by ^{40}Ar – ^{39}Ar and ^{87}Rb – ^{86}Sr . The present zircon ^{207}Pb – ^{206}Pb age is the first direct zircon age determination of the Imbrium impact event from an Apollo sample. Previous measurements of zircon ages of Apollo IMBs have recorded events pre-dating the Imbrium basin-forming event.

© 2011 Elsevier B.V. All rights reserved.

1. Introduction

Rock and mineral fragments and impact-melts contained in lunar impact breccias carry a textural and isotopic record of the complex history of shock and heating events involved in their formation. The Apollo 12 landing site was in the Imbrium–Procellarum region (known as the Procellarum KREEP Terrane or PKT), which is distinctive because of the high content of KREEP (K, rare earth elements, P, as well as other incompatible elements such as Zr, Th, U, etc.) of the nonmare materials at the surface, as shown in Apollo and Lunar Prospector gamma-ray spectrometer data (Elphic et al., 2000; Feldman et al., 1999; Lawrence et al., 1998, 2000; Reedy, 1978). Thus KREEP-rich impact-melt breccias (IMBs) record important information about the internal and thermal evolution of the Moon.

The U–Pb isotopic system in zircon grains is likely the geochronological system most resistant to shock metamorphism and we have applied this technique to investigate the age of formation and the correlation of Th- and U-rich IMBs in lunar meteorite SaU (Sayh al Uhaymir) 169 and similar small rock fragments discovered in soils from

the Apollo 12 landing site (Fig. 1; Korotev et al., 2011). Our results have implications for the correlation and formation of Th-rich IMBs, the origin of the impact melt, the age of the Imbrium impact event, and of events that predate and post-date the period of impact-basin formation as recorded on the Moon.

2. Samples and analytical methods

Apollo 12 high-Th IMB rock fragments were mounted on two separate polished microprobe thick-section mounts. In one section, we mounted seven chips from five different Apollo 12 high-Th IMB fragments: 12032,366-2; 12032,366-10a; 12032,366-10b; 12033,624-24; 12033,634-29; 12033,638-1a1; and 12033,638-1a2. Each of the rock fragments in this section was irradiated for instrumental neutron activation analysis (INAA) as described in Korotev et al. (2011). In the second section, we mounted a large, unirradiated chip of sample 12033,638-1c (from the same rock fragment as 12033,638-1a1 and ,638-1a2). Photos showing the Apollo 12 rock fragment sample mounts are in an on-line supplemental file (Fig. S-1). We also investigated zircons in several IMB chips from the SaU 169 lunar meteorite. Four chips about 4 mm across of SaU 169 were included on one polished microprobe thick-section mount (Fig. S-2).

* Correspondence author. Tel.: +1 636 675 2436.

E-mail address: blj@wustl.edu (B.L. Jolliff).

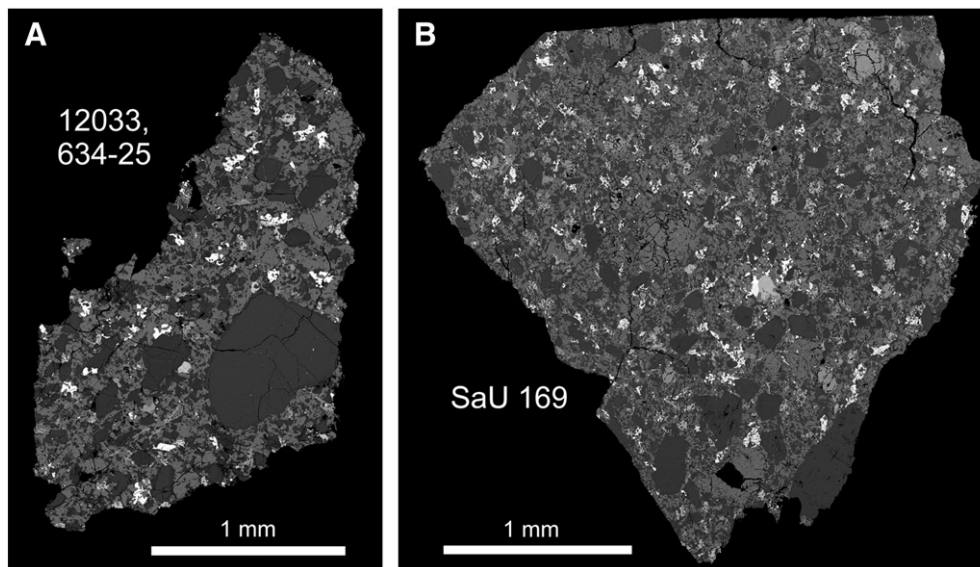


Fig. 1. Backscattered-electron images of (A) Apollo 12 high-Th IMB 12033,634-25 and (B) the IMB lithology in lunar meteorite SaU 169. Both rocks contain calcic plagioclase clasts (dark gray; An_{95}) in a matrix dominated by more sodic plagioclase (An_{55-80}) and pyroxene (medium gray; $En_{61-68}Wo_{.7}$), and abundant accessory phases (typically light gray to white): K-feldspar, apatite, RE-merrillite, ilmenite, zircon, baddeleyite, and troilite. SaU 169 contains a small amount of olivine (e.g., large grain, upper right), which is slightly brighter than pyroxene.

For petrographic characterization of samples, we used the JEOL 8200 electron microprobe at Washington University. Mineral compositions were determined by wavelength-dispersive X-ray analysis. Zircons were located using a combination of backscattered-electron (BSE) images and X-ray images obtained through a combination of wavelength and energy dispersive spectrometers.

Major and trace-element compositions were determined by a combination of INAA (Korotev, 1991; Korotev et al., 2011) and fused bead analysis by EPMA (electron probe microanalysis) as described in Zeigler et al. (2005) and Korotev et al. (2011). Average compositions from these analyses are shown in Table 1.

Sample mounts for SHRIMP analysis were coated with gold and U–Pb measurements done on the SHRIMP II at the Beijing SHRIMP Center following established operating procedures described by Williams (1998). The standard Ceylon zircon BR266 (Stern, 2001) was analyzed on a separate mount, and standard analyses were made preceding and alternately during analyses of the unknowns. The analytical spot size was 12 μm for SaU 169, fragment 12033,638-1c and a few other analyses (634-25-1.1; 366-10a-3.1, 7.1, 9.1, 9.2, 10.1); the spot size was 8 μm for all other analyses. The primary current was 1 nA. Each spot was rastered for 8–10 min prior to analysis and five scans were made for each age determination. The common Pb correction used was from the model of Stacey and Kramers (1975) assuming that the major contribution of common Pb was derived from sample processing. This assumption follows the experience of Nemchin et al. (2008). The SQUID and ISOPLOT programs were used to process the SHRIMP-II data. The uncertainties for individual analyses in Tables 2 and 3 are given at the 1-sigma level, whereas the uncertainties on weighted mean $^{207}\text{Pb}/^{206}\text{Pb}$ values in the text are given at the 2-sigma level.

3. Sample descriptions

3.1. Sayh al Uhaymir 169 lunar meteorite

Lunar meteorite SaU 169, found in the Sultanate of Oman (Russell et al., 2003), is an unusual dilithologic meteorite, consisting of a fine-grained polymict IMB partially rimmed by shock-lithified regolith. The IMB lithology in SaU 169 has been described by Gnos et al. (2004) as a holocrystalline, fine-grained polymict breccia consisting of shocked igneous rocks and mineral clasts in fine-grained

Table 1

Compositions of impact-melt breccias and KREEP.

Column notes	KREEP IMB					Avg mafic	KREEP
	A12	A12	SaU	A 14	A14	IMB	Av
	Typical	High-Th	169	Typical	Th > 24		High-K
	1	2	3	4	5	6	7
SiO ₂	49.2	47.5	45.5	48.8		47.17	50.3
TiO ₂	1.62	2.33	2.3	1.7		1.39	2.0
Al ₂ O ₃	16.9	15.3	15.2	16.6		18.1	15.1
Cr ₂ O ₃	0.19	0.13	0.13	0.18	0.16	0.21	0.2
FeO	10.0	10.8	11.4	10.3	10.3	9.24	10.3
MnO	0.14	0.13	0.15	0.13		0.12	0.13
MgO	8.9	10.3	10.8	10.1		11.34	8.29
CaO	10.2	9.66	11.1	9.90	10.2	11.0	9.79
Na ₂ O	0.95	1.07	0.87	0.82	0.88	0.68	0.94
K ₂ O	0.73	0.52	0.41	0.72		0.41	0.96
P ₂ O ₅	0.73	1.14	1.32	0.5		0.43	0.80
Sum	99.6	98.9	99.2	99.2		100.1	98.8
Mg/(Mg + Fe)	0.61	0.63	0.63	0.64		0.69	0.59
Sc	21.6	23.5	25.8	20.9	24.2	17.7	23
Co	25.9	22.5	30.2	33.6	27.7	34.1	25
Ni	192	166	252	335	247	369	–
Sr	204	221	310	184		178	200
Zr	1240	2240	2260	1300	2108	780	1400
Cs	0.72	0.70	0.52	0.84	1.19	0.46	1.0
Ba	993	1430	1285	970	1366	575	1300
La	90.2	166	172	87.4	139	57.5	110
Ce	230	417	436	224		149	280
Nd	135	242	258	135		88	178
Sm	39.3	70.5	74.8	38.5	60.9	25.8	48
Eu	3.14	4.01	3.95	2.71	2.75	2.16	3.3
Tb	7.94	14.3	15.2	7.63	12.3	5.21	10
Yb	28.6	52.6	54.8	27.9	43.7	18.0	36
Lu	3.92	7.15	7.5	3.82	5.97	2.48	5
Hf	30.4	53.1	52.4	30.4	50	19.7	38
Ta	3.7	6.7	6.5	3.7	5.9	2.35	5
Th	16.4	30.4	30	17	28	9.95	22
U	4.6	8.0	7.9	4.6	7.5	2.73	6.1

Notes:

Oxide concentrations are in weight percent; others are in ppm. Mg/(Mg + Fe) is molar. Columns 1–3 are from Korotev et al., 2011; Column 4 is from Jolliff, 1998.

Column 5, Th > 24 ppm, is from data reported by Jolliff et al., 1991; average is for 5 samples, all INAA.

Column 6 is average of compositions in Table 1, Jolliff, 1998, plus the two Ap 12 compositions in this table.

Column 7 is from Warren, 1989.

Table 2
SHRIMP Zircon Pb–Pb results for Apollo 12 IMB rock fragments.

Frag no.	U (ppm)	Th (ppm)	Th/U	% ²⁰⁶ Pbc	²⁰⁷ Pbr/ ²⁰⁶ Pbr		²⁰⁷ Pbr/ ²³⁵ U		²⁰⁶ Pbr/ ²³⁸ U			²⁰⁶ Pb/ ²³⁸ U Age		²⁰⁷ Pb/ ²⁰⁶ Pb Age		% discordant	Overlap	
					²⁰⁴ Pb-corr	±% err	²⁰⁴ Pb-corr	±% err	²⁰⁴ Pb-corr	±% err	Err corr	²⁰⁴ Pb-corr	±1σ err	²⁰⁴ Pb-corr	±1σ err			
Apollo 12 IMB fragments																		
12033, 634-29																		
7.1	174	51	0.30	2.50	0.3944	1.69	43.5	3.3	0.800	2.8	0.858	3790	81	3888	25	4	0.25	
12033, 638-1A																		
1A1-2.1	144	51	0.36	1.40	0.4120	1.79	51.0	4.0	0.898	3.6	0.894	4130	109	3953	27	−4	0.20	
1A2-1.1	267	294	1.14	2.61	0.3971	1.54	44.6	3.1	0.814	2.7	0.871	3840	79	3898	23	3	0.25	
1A2-3.1	163	78	0.50	1.57	0.3953	1.59	47.8	3.7	0.876	3.3	0.901	4056	99	3891	24	−3	0.25	
12033, 638-1C																		
2.1	167	121	0.75	0.15	0.4769	0.48	60.5	2.4	0.920	2.4	0.981	4203	74	4171	7	−1	0.00	
1.2	60	24	0.41	0.36	0.4116	0.89	47.8	2.4	0.843	2.2	0.930	3934	66	3952	13	0	0.10	
1.3	112	50	0.46	0.34	0.3985	0.70	52.2	2.2	0.950	2.1	0.949	4299	66	3903	11	−10	0.25	
4.1	144	97	0.70	0.26	0.4026	0.58	43.5	2.0	0.783	1.9	0.956	3724	54	3919	9	5	0.00	
12032, 366-10																		
10B-1.1	162	81	0.52	2.09	0.4048	2.16	47.4	4.2	0.850	3.6	0.857	3965	106	3927	33	0	0.00	
10A-3.1	468	373	0.82	0.23	0.3986	0.59	47.9	1.9	0.871	1.8	0.950	4034	54	3904	9	−3	0.00	
10A-3.1S	519	425	0.85	0.05	0.3968	0.80	50.7	2.2	0.927	2.1	0.932	4227	64	3897	12	−8	0.00	
10A-9.2	489	339	0.72	0.28	0.4020	0.42	44.4	1.8	0.802	1.7	0.972	3790	50	3917	6	3	0.20	

crystalline matrix. The mineral chemistry of lithic clasts and mineral clasts suggests that the impact target area consists predominantly of norite and olivine norite. Other lithic components include granitoid and granulitic clasts, but no highland anorthosites (Gnos et al., 2004). Very small zircon grains occur in the matrix and constitute an ideal means to date the meteorite because most of them appear to have crystallized from the matrix melt. The IMB in this meteorite is richer in KREEP elements than any other known lunar IMB (Gnos et al., 2004). Relative to typical Apollo KREEP-rich IMBs such as average Apollo 14 IMB, the IMB in SaU 169 is richer in the high field-strength trace elements (HFSE), such as REEs, Zr, Hf, Ta, U, and Th by a factor of ~2, but Ba is less enriched and the large alkali elements, represented in our analyses by K and Cs, are somewhat depleted (Table 1, Fig. 2).

On the basis of its high Th concentration (33 ppm), Gnos et al. (2004) argued that SaU 169 almost certainly originated from within one of the Th hot spots on the Moon, identified by the global gamma-ray and neutron spectrometer mapping done by the Lunar

Prospector Mission (Lawrence et al., 1998). Most significantly, Gnos et al. reported ²⁰⁷Pb/²⁰⁶Pb ages on 12 poikilitic zircons from the crystallized impact melt that yield a weighted average age of 3909 ± 13 Ma (2σ; MSWD = 0.33). They interpreted this age as dating the crystallization of the impact melt and ascribed the impact melt to formation during the Imbrium basin-forming event. This age is significantly older than the previously accepted best estimate of the ages of 3.85 ± 0.02 Byr for the Imbrium and 3.89 ± 0.01 Byr for the Serenitatis basin (Dalrymple and Ryder, 1996; Stöffler and Ryder, 2001; Stöffler et al., 2006). However, this age is slightly younger than the U–Pb age of 3926 ± 3 Ma reported for apatite from Apollo 14 breccias (Nemchin et al., 2009).

3.2. Apollo 12 impact-melt breccias

Although the Apollo 12 landing site is in Mare Insularum and is immediately underlain by basalt, there is a considerable proportion of nonmare materials in the regolith samples collected during the

Table 3
SHRIMP zircon Pb–Pb results for the IMB lithology of lunar meteorite SaU 169.

Frag no.	U (ppm)	Th (ppm)	Th/U	% ²⁰⁶ Pbc	²⁰⁷ Pbr/ ²⁰⁶ Pbr		²⁰⁷ Pbr/ ²³⁵ U		²⁰⁶ Pbr/ ²³⁸ U			²⁰⁶ Pb/ ²³⁸ U age		²⁰⁷ Pb/ ²⁰⁶ Pb age		% discordant	Overlap	
					²⁰⁴ Pb-corr	±% err	²⁰⁴ Pb-corr	±% err	²⁰⁴ Pb-corr	±% err	Err corr	²⁰⁴ Pb-corr	±1σ err	²⁰⁴ Pb-corr	±1σ err			
Meteorite SaU 169 IMB																		
Fragment 1																		
Z1-1.1	171	147	0.89	1.66	0.3958	0.71	45.1	2.5	0.826	2.4	0.958	3883	69	3893	11	0	0.00	
Z1-1.2	234	288	1.27	0.47	0.3995	0.59	46.9	2.4	0.851	2.4	0.970	3968	70	3907	9	−2	0.00	
Z1-1.3	294	268	0.94	0.30	0.3965	0.60	47.5	2.9	0.869	2.8	0.978	4031	85	3896	9	−3	0.10	
Fragment 2																		
Z2-1.1	161	118	0.76	0.61	0.4049	0.70	50.1	2.5	0.897	2.4	0.961	4129	74	3927	10	−5	0.05	
Z2-1.2	264	187	0.73	0.22	0.4021	0.60	49.3	2.6	0.888	2.5	0.972	4098	75	3917	9	−5	0.15	
Z3-1.1	228	242	1.09	0.55	0.4052	0.63	50.8	2.5	0.909	2.4	0.968	4169	74	3928	9	−6	0.20	
Z3-1.2	208	193	0.96	0.35	0.4029	0.61	48.3	2.6	0.869	2.5	0.971	4032	75	3920	9	−3	0.05	
Fragment 4																		
Z4-1.2	202	118	0.60	0.54	0.4062	0.57	46.4	2.4	0.828	2.3	0.972	3889	69	3932	9	1	0.00	
Z4-1.3	200	35	0.18	0.27	0.4099	0.56	50.6	2.4	0.895	2.4	0.973	4119	72	3946	8	−4	0.20	

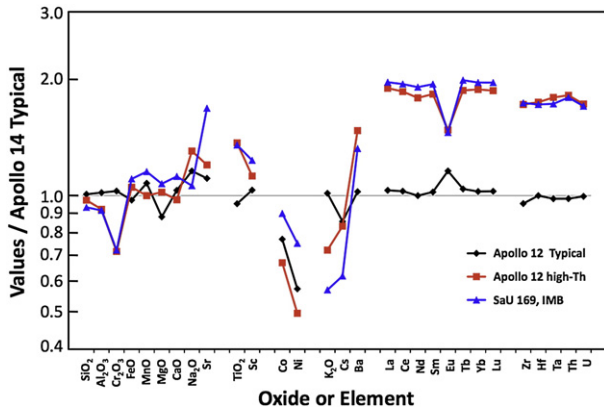


Fig. 2. Elemental and oxide concentrations of Apollo 12 IMBs and SaU 169 IMB normalized to typical Apollo 14 IMB (values from Jolliff et al., 1991). For typical Apollo 12 IMB, the average composition is very similar to that of Apollo 14 IMBs. However, for the high-Th IMBs from Apollo 12 and the SaU 169 meteorite, most of the incompatible trace elements are enriched by nearly a factor of 2, with the exception of the large alkali elements K and Cs, and the patterns for the Apollo 12 high-Th IMB average composition and the SaU 169 IMB are very similar to each other. The main exception is Sr, which is high in SaU 169 owing to terrestrial contamination.

Apollo 12 mission (Korotev et al., 2011). These nonmare materials consist mainly of KREEP-rich IMBs and ropy glass, with minor feldspathic components, granitic components, and other breccia lithologies (Korotev et al., 2011). Most IMBs from Apollo 12 regolith samples have a similar composition to those of Apollo 14 and the group-1 IMBs of Apollo 15 (Korotev, 2000; Korotev et al., 2011; Ryder and Spudis, 1987), differing mainly in subtle trace-element patterns (Fig. 2), so IMBs with this typical composition are considered to be the typical Apollo 12 KREEP IMBs by Korotev et al. (2011). Although these IMBs vary somewhat in composition, they are all rich in incompatible trace elements, and the average composition is very similar to the composition of the Apollo 12 KREEP-rich ropy glasses (Korotev et al., 2011).

Recently, a new group of clast-bearing, crystalline-matrix IMBs with exceptionally high incompatible trace element concentrations (e.g., 30 ± 2 ppm Th; Fig. 3) was recognized in the Apollo 12 regolith and has been referred to as high-Th IMBs (Korotev et al., 2011; Zeigler et al., 2006). Among 115 KREEP-rich rock fragments from Apollo 12 soils analyzed by Korotev et al. (2011), 12 rock fragments showed

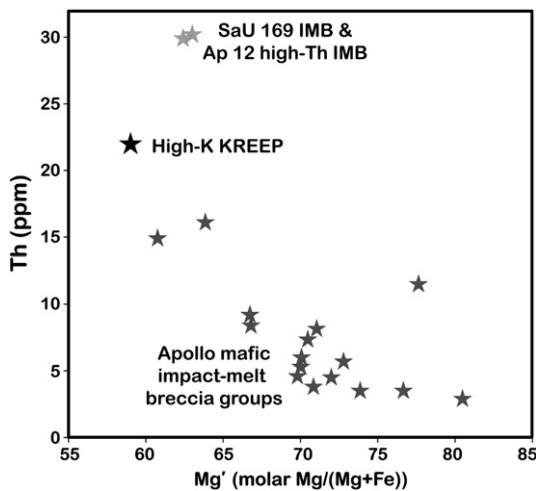


Fig. 3. Apollo 12 high-Th IMB and SaU 169 IMB have very similar chemical compositions. Plot compares average Mg' values and Th concentrations of Apollo 12 and SaU 169 high-Th IMBs to other Apollo IMB groups (average compositions) and "average high-K KREEP" (Warren, 1989). Symbols for A12 and SaU 169 IMBs are artificially offset; otherwise they plot too close to each other to distinguish on this scale.

this high-Th concentration. Most of these rock fragments come from soils 12032 and 12033, which were collected from a 15-cm-deep trench inside the north rim of Head Crater (Warner, 1971). Relative to the typical Apollo 12 soils, 12032 and 12033 are less basaltic and richer in components of KREEP-rich IMBs, alkali anorthosite, and granitic materials.

The different fragments of Apollo 12 high-Th IMB all have similar textures, mineral assemblages, compositions, and clast populations, as first reported by Zeigler et al. (2006). These rock fragments consist of irregularly shaped lithic and mineral clasts, set in a fine-grained recrystallized matrix consisting of low-Ca pyroxene (En_{61-69}, Wo_{2-7}), sodic plagioclase (An_{55-80}), and minor amounts of ilmenite, RE-merrillite, apatite, and barian K-feldspar, as well as trace amounts of zircon and baddeleyite. The texture of the fine-grained matrix is subophitic to micro-poikilitic. Mineral clasts are dominated by calcic plagioclase (typically $>An_{90}$) and minor pyroxene. Plagioclase clasts have rims of more sodic plagioclase indicating marginal reaction with melt. Lithic clasts are dominated by plagioclase ($An_{79-90}Or_{0.8}$) with minor pyroxene ($En_{44-61}Wo_{4-41}$) and are mainly recrystallized.

The lithology of the Apollo 12 high-Th IMBs is very similar to the lithology of IMB portions of meteorite SaU 169 (Fig. 1). In SaU 169, irregular lithic and mineral clasts are set in a fine-grained crystalline matrix, which consists mainly of low-Ca pyroxene (En_{61-64}, Wo_{2-4}) and interstitial plagioclase, with minor K-feldspar, poikilitic ilmenite, RE-merrillite, zircon, and apatite. Most mineral clasts are calcic plagioclase, locally associated with pyroxene. SaU 169 contains a small amount of olivine, consistent with its olivine-normative bulk composition, whereas the Apollo 12 samples are olivine-free. Neither the Apollo 12 IMBs nor the SaU 169 IMB contain lithic or mineral clasts associated with ferroan anorthosite.

The geochemistry of the Apollo 12 high-Th IMBs is nearly identical to that of the SaU 169 IMB (Korotev et al., 2011). In fact, the difference in the average compositions of the Apollo 12 high-Th and SaU 169 IMBs is less than the compositional variability observed in individual fragments of the Apollo 12 group or subsamples of SaU 169. Concentrations of HFSE in Apollo 12 high-Th (and SaU 169) IMBs are ~2 times higher than in typical Apollo 12 IMBs, e.g., the average concentrations of Zr, Sm, Yb and Th are 2202, 69, 52, and 30 ppm, respectively, whereas the corresponding concentrations in typical Apollo 12 IMBs are 1240, 39, 29, and 16, respectively (Table 1, Fig. 2). On the other hand, the large alkali elements K and Cs are depleted, whereas Ba and Sr are moderately enriched, forming an unusual separation of the large-ion lithophile elements (LILE), seen also in SaU 169 (Fig. 2). The contents of major elements and compatible trace elements in Apollo 12 high-Th IMBs are also very similar to those in SaU 169 and differ from the other Apollo IMBs (e.g., Fig. 3). The high-Th IMB group is at the FeO-rich end (10.6 wt.%) of the IMB compositional range and also has elevated Ti and Sc compared to average Apollo 14 IMB. The bulk Mg' (molar $Mg/(Mg + Fe) \times 100$) of the high-Th IMB group is ~63, which is low among the mafic IMBs (Fig. 3). The inter-element ratios among the ITEs are generally in KREEP-like proportions, albeit at $\sim 1.5 \times$ the level of high-K KREEP (Warren, 1989). The alkali and alkaline-earth elements are not as enriched as they are in high-K KREEP, however. For example, the K_2O in the high-Th IMBs (0.5 wt.%) is lower than typical Apollo 12 IMBs (0.7 wt.%), but similar to SaU 169 (0.4 wt.%).

The similarities in composition and lithology between SaU 169 IMB and the Apollo 12 high-Th IMBs provide a clear connection between the SaU 169 lunar meteorite and the Apollo samples. In following sections, we investigate the ages of these samples by analyzing their zircons and we consider possible origins.

4. Results

In the following section we present descriptions of the zircon grains and SHRIMP-II U-Pb age determinations on the zircons. We

discuss the implications of the results in terms of the correlation of the Apollo 12 high-Th IMB rock fragments with SaU 169 and the possible origins as basin-derived impact melt.

4.1. Description of zircons in Apollo 12 high-Th impact-melt breccias

In the high-Th IMBs from soils 12032 and 12033, the matrix minerals have irregular and rounded shapes with embayed crystal boundaries. Zircon grains are small, generally irregular-tabular to elongate in shape, and have rounded boundaries with adjacent minerals, although rare grains are composite forms that have a combination of rounded boundaries and straight crystal faces (Fig. 4A–C). The zircon grains are generally interstitial, reflecting late-stage crystallization and are commonly intimately intergrown with ilmenite. The irregular, and in some cases skeletal and elongate forms, rarely

have accessible surface widths more than $\sim 20\ \mu\text{m}$ (Fig. 4A). Most grains appear to be in cogenetic equilibrium with surrounding minerals in the crystalline matrix and imply that they crystallized from the impact melt. Several grains with irregular tabular forms and rounded terminations, however, appear to be inherited mineral clasts (Fig. 4C).

4.2. Description of zircons in the SaU 169 impact-melt breccia

Zircon grains, identified in the polished SaU 169 chips from BSE imagery, are small with irregular shapes ranging from rounded, broadly tabular and indented grains (Fig. 4D, E) to sieve-texture crystals, such as the grain shown in Fig. 4F, which forms a poikilitic, branching, interstitial network, and is unlike any occurrence seen in terrestrial rocks. This morphological type is referred to as morphology

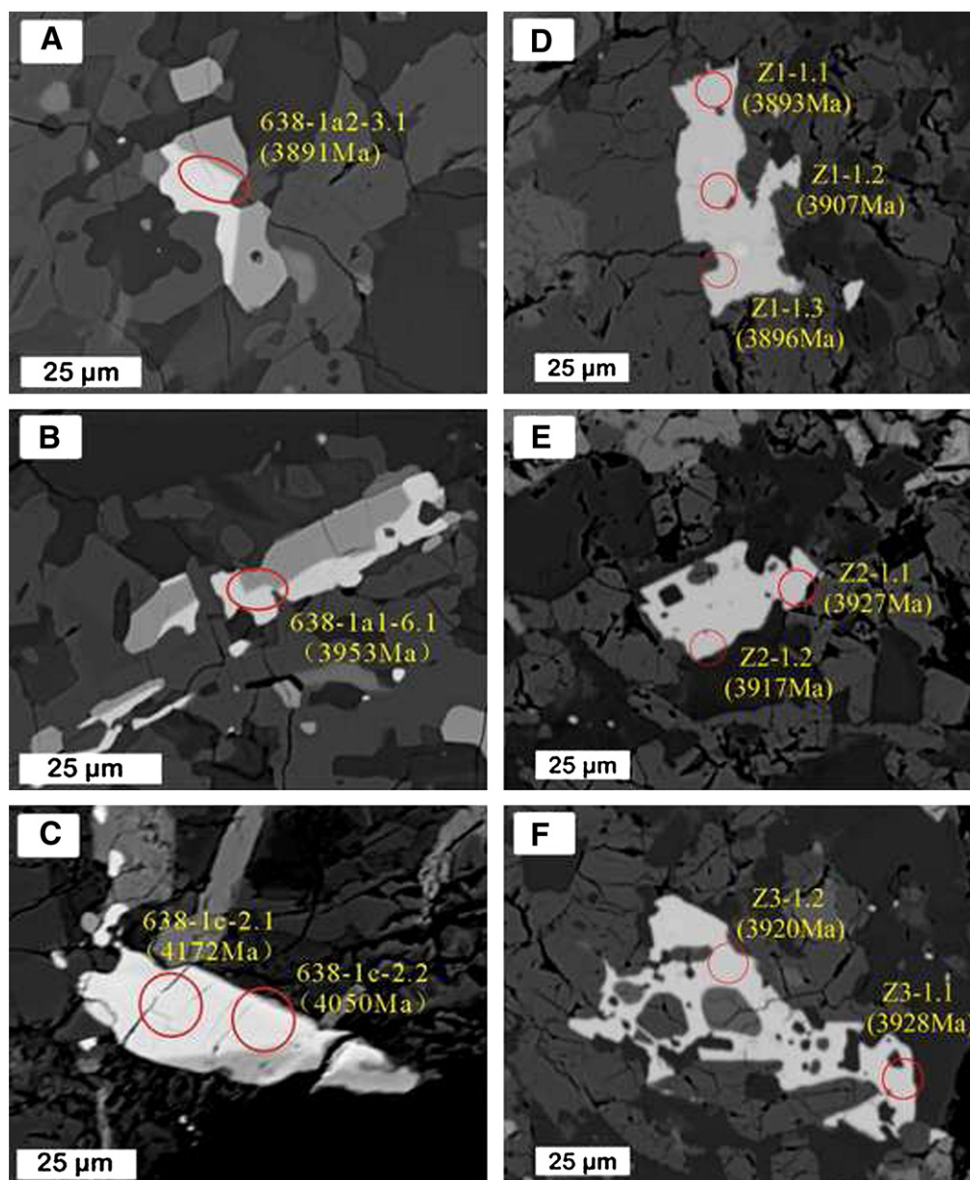


Fig. 4. Examples of zircon grains analyzed in this study (BSE). (A, B, C) Zircon grains in Apollo 12 IMB; plagioclase is dark gray, pyroxene is intermediate gray, and ilmenite is light gray and intergrown with zircon (white). (A) Interstitial, irregular triangular shaped grain with combined rounded and straight crystal face boundaries with adjacent grains; intergrown with ilmenite. (B) Elongate irregular-shaped grain with rounded indented grain boundaries intimately intergrown with ilmenite. (C) Irregular-shaped rectangular inherited grain with rounded terminations. (D, E, F) Zircon grains from the IMB lithology of lunar meteorite SaU 169; plagioclase is dark gray, pyroxene, intermediate gray, and olivine, light gray. (D) Approximately rectangular zircon grain intergrown with pyroxene. (E) Rectangular grain with rounded, embayed and straight crystal-face boundaries with adjacent grains. (F) Poikilitic zircon penetrating surrounding pyroxene and plagioclase, and enclosing small silicate mineral grains. Ages noted in parentheses are ^{204}Pb -corrected $^{207}\text{Pb}/^{206}\text{Pb}$ ages (Tables 2 and 3).

type 7 by Nemchin et al. (2008) and described as a “poikilitic impact-melt zircon formed during equilibrium crystallization of the impact melt.” We have not seen similar development of this texture in zircons from the Apollo 12 IMB sections. Also, the intimate association of anhedral zircon and ilmenite (e.g., Fig. 4A, B) observed in the IMBs from Apollo 12 is not as frequently observed in zircons from the IMB lithology of SaU 169.

4.3. Geochronology of zircons in Apollo 12 high-Th impact-melt breccias

We analyzed 42 spots on zircon grains in 5 different high-Th IMB fragments from soils 12032 and 12033. Thirty-eight analyses align along a discordant line with an intercept age of 3913 ± 10 Ma, whereas four analyses on three grains produce older ages ranging from 4.0 to 4.2 Ga (Fig. 5). Among these data, however, we observe cases of both normal and reverse discordance. Below we consider possible causes of the discordance as well as our approach to treating and interpreting the data.

Our analyses were made using an 8–12 μm spot on very small, irregular shaped grains (Fig. 4). In so doing, we found it difficult to avoid overlap onto adjacent mineral phases. Substantial overlap resulted in calibration problems (see below) leading to uncontrolled apparent normal and reverse discordance. It is also possible that this effect was aggravated by a contribution of unsupported lunar Pb from overlapped grains. Another potential problem in these analyses is possible edge effects. There have been a number of reports of a lowering of $^{207}\text{Pb}/^{206}\text{Pb}$ ages in the outer 1 μm or less of zircon grains (e.g., Trail et al., 2007).

To minimize potential effects of discordance on our results, we exclude analyses with the most discordance ($> 10\%$ discordance) and spots with the most overlap onto adjacent grains (more than 25%) and report the analyses in Table 2, where % overlap was estimated from BSE images obtained after ion-microprobe spot analyses. This exclusion yields 12 analyses that are the most concordant and these data are presented on a Concordia plot in Fig. 6A. Most data points are concordant within the uncertainties or slightly reversely discordant. We attribute the reverse discordance to calibration problems mainly associated with comparing samples and standards in different mounts. Data for all analyzed points are given in a table in the on-line supplement (Table S-1).

The zircon ages fall into two groups. The main group of 11 analyses yields a mean $^{207}\text{Pb}/^{206}\text{Pb}$ age of 3914 ± 7 (2σ) Ma with a MSWD of 1.8 and an intercept age of 3913 ± 19 Ma (MSWD = 1.6), which is identical with the intercept age of all 38 analyses (3913 ± 10 Ma). The excluded analyses, taken together, yield an intercept age of 3916 ± 13 Ma. Our preferred age is 3914 ± 7 Ma on the basis of the best data. We interpret this age as the crystallization age of

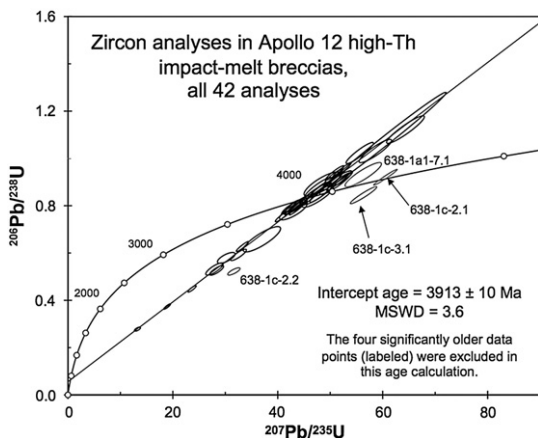


Fig. 5. Concordia plot of all SHRIMP U–Pb analyses of Apollo 12 high-Th IMBs, excluding only the four analyses labeled and plotted with grayed ellipses.

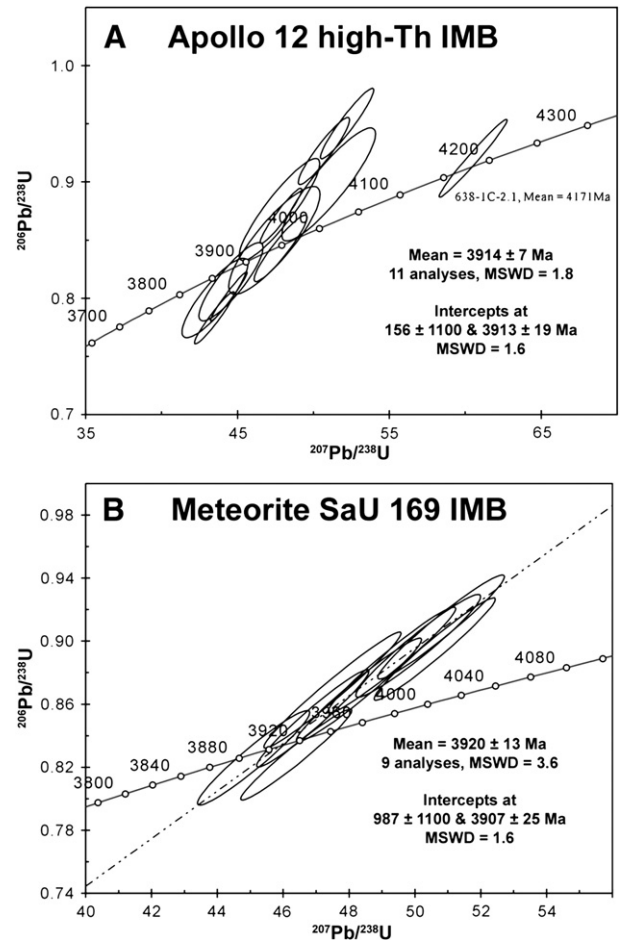


Fig. 6. Concordia plots of SHRIMP U–Pb analyses of (A) analyses on zircons from the IMB fragment from Apollo 12 with $\leq 25\%$ overlap with neighboring grains, and (B) analyses on zircons from the IMB portion of lunar meteorite SaU 169.

the melt and thus the age of the impact event that formed these impact-melt breccias. The second group consists of analyses that yield older ages, represented by concordant analysis 638-1c-2.1 (Fig. 6A), which has a $^{207}\text{Pb}/^{206}\text{Pb}$ age of 4171 ± 7 Ma (1σ). This zircon grain has a tabular, sub-prismatic shape with rounded terminations, suggesting reaction with the impact melt prior to crystallization of the matrix and thus an inherited origin. The U and Th contents of the concordant grains having $\leq 25\%$ overlap were 60–489 ppm and 24–425 ppm, respectively. A table with $^{207}\text{Pb}/^{206}\text{Pb}$ analyses of all analyzed grains is provided in supporting documentation.

4.4. Geochronology of zircons in SaU 169

SHRIMP-II U–Pb analyses of the zircon grains were made using a reduced, 12 μm primary beam analysis spot. Results of nine SHRIMP-II U–Pb analyses are included in Table 3 and shown on a Concordia plot in Fig. 6B. Data for all analyzed points are given in a table in the on-line supplement. The small reverse discordance is attributed to calibration errors resulting from the sample and standard being on separate mounts. No zircon grains with inherited radiogenic Pb were identified. The combined $^{207}\text{Pb}/^{206}\text{Pb}$ age of all analyses is 3920 ± 13 Ma (2σ , MSWD 3.6) and this age is interpreted to date the crystallization of the melt. This age is identical within uncertainty to the age of 3914 ± 7 Ma for zircons from the IMB in the Apollo 12 IMB fragments. Also, the range of U and Th contents of zircons from the high-Th IMB from SaU 169, of 171–294 ppm and 35–288 ppm, respectively, are broadly similar to U and Th of the Apollo 12 IMB zircons of 60–489 ppm and 24–425 ppm, respectively. These results

and the broadly similar zircon morphological features support the conclusion of Korotev et al. (2011) that SaU 169 IMB and the high-Th Apollo 12 IMB are different samples of a single unit of IMB.

5. Discussion

5.1. The distribution of high-Th melts

The IMB samples with exceptionally high Th represent a new lunar IMB type. The U and Th contents in zircons of the Apollo 12 high-Th IMBs provide some constraints on the origin of the zircon grains, themselves, and the matrix melt. U and Th concentrations in these zircons are similar to those in zircons from lunar granophyres (Meyer et al., 1996) but are generally higher than the concentration of these elements in >4 Ga zircons that form cogenetic minerals in noritic clasts and that occur as mineral clasts in the matrices of breccias from Apollo 14 and Apollo 17 (Nemchin et al., 2008, 2009). The few inherited zircons in the Apollo 12 IMBs also have similar U and Th contents, raising the question of whether the present high-Th melt was produced by closed-system melting of an original source where a few zircons survived or whether the melt represents an influx of KREEP materials into an older source rock which was itself KREEP rich. The presence of calcic plagioclase clasts rimmed by more sodic plagioclase and the presence in the IMB equilibrium assemblage of more sodic plagioclase suggest that the high-Th material was mixed with less evolved primary rocks during the basin impact event. The actual source location of the Apollo 12 high-Th IMB regolith fragments is uncertain as they may have been transported to the present location by a number of impact ejection events.

Gnos et al. (2004) proposed that the SaU 169 meteorite derived from a location near Lalande Crater, which impacted into and excavated Th-rich deposits (Fig. 7), possibly themselves derived from Imbrium. Presumably the meteorite would have been ejected from a small, recent crater in the proximal Lalande ejecta. The similarity of SaU 169 and the Apollo 12 high-Th IMBs in texture, geochemistry and geochronology, however, supports a common origin. The fact that the Apollo 14 site lies between Lalande Crater and the Apollo 12 site, yet the Apollo 14 samples do not to our knowledge contain this particular high-Th IMB lithology (e.g., Jolliff et al., 1991; Korotev et al., 2011; Table 1, Col. 5), suggests that the primary source of the IMBs may be one from which samples were delivered to the Apollo 12 site, but not Apollo 14. We suggest that the high-Th character of the meteorite SaU 169 only reflects its affinity with the specific deposits that were excavated and delivered to the Apollo 12 site and the launch site of SaU 169. The source could be widespread with more than one location, but the absence of the high-Th IMBs from Apollo 14 and Apollo 15 samples indicates that it could also be localized. It is possible that the source was in the vicinity of Copernicus Crater, from which the high-Th IMBs would have been delivered to the Apollo 12 site by visible ray material (Fig. 7). As pointed out by Korotev et al. (2011), Apollo 12 KREEP-rich nonmare components could have derived from other large craters such as Reinhold or Lansberg, which, although older than Lalande, also impacted Th-rich deposits that are likely Imbrium ejecta (Wilhelms, 1987). If the high-Th impact-melt breccias of Apollo 12 and lunar meteorite SaU 169 represent the same unit of impact melt, then it seems more likely that they come from north of the Apollo 12 site (i.e., between Apollo 12 and Imbrium basin) and less likely that they come from the Lalande region east of Apollo 14. Moreover, the relatively coarsely

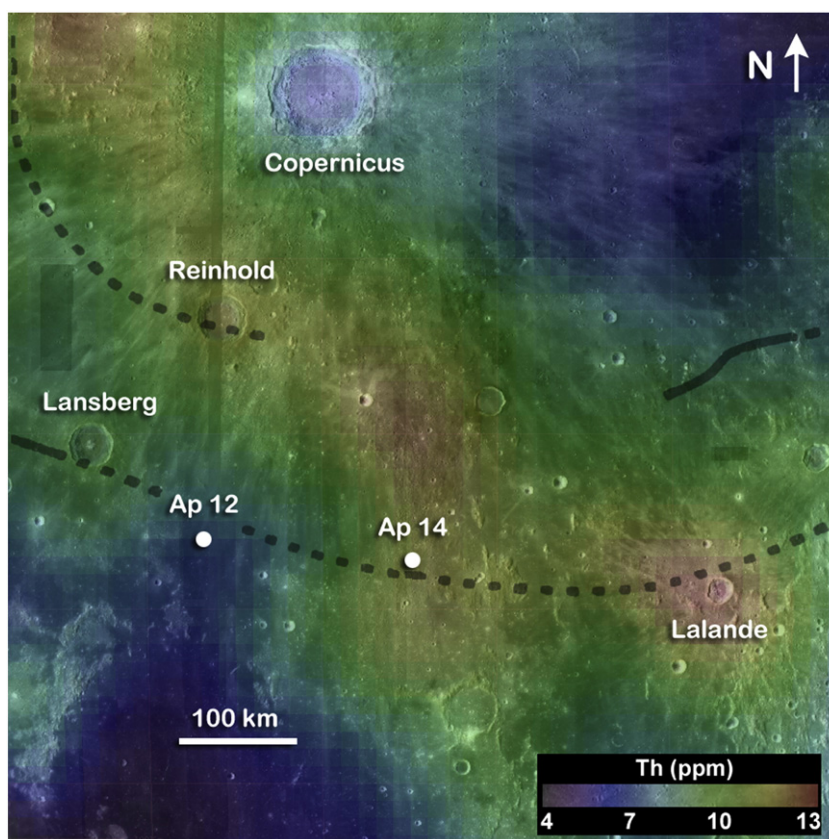


Fig. 7. Map of the Apollo 12–Apollo 14 region made by overlaying a Th concentration map (half degree binned, data from Lawrence et al., 2000) on a composite LRO Wide Angle Camera (Robinson et al., 2010) and Clementine UVVIS mosaic. Hot colors (red) represent the highest Th concentration and cool colors, the lowest Th. Impact craters referred to in text are labeled. Dashed dark gray lines represent the possible trace of Insularum basin rings, from Wilhelms (1987), Plate 3. Projection is sinusoidal.

crystalline matrix of the high-Th IMBs suggests crystallization in a large, proximal melt deposit or in the basin interior melt sheet, itself. Again, a more likely source would be materials in the region excavated by Copernicus.

5.2. Implication of the new age determinations

Gnos et al. (2004) reported $^{207}\text{Pb}/^{206}\text{Pb}$ zircon ages of 3909 ± 13 Ma for the meteorite SaU 169 and suggested it represented an accurate determination of the age of Imbrium impact event. In the following discussion, we consider, in addition to an Imbrium origin, whether the impact event that formed these IMBs might have been an event older than Imbrium such as Insularum, Humorum, Nubium, or Serenitatis. Given that we have samples with potentially diverse sites of origin (Apollo 12 and the SaU 169 source crater), we consider it most likely that these IMBs formed in a basin impact event.

The Apollo 12 soil components reported by Korotev et al. (2011) consist of about one third nonmare materials even though the Apollo 12 landing site is located on the mare basalt surface. The nearby highlands are dominated by the Fra Mauro Formation, which is a facies of Imbrium basin ejecta deposits (Wilhelms, 1987). Some of the younger, moderate-sized impacts that formed craters into Imbrium ejecta deposits, such as Copernicus and Reinhold (Fig. 7), possibly redistributed ejecta to the area of the Apollo 12 landing site; however, the ages of the zircon grains preclude the possibility that the IMBs in 12032 and 12033 are impact melt from these younger impacts, themselves. It is more likely that one of these impacts excavated a basin impact-melt deposit and simply delivered the breccias to the Apollo 12 site.

The KREEP-rich (and especially the Th-rich) composition of the high-Th IMBs (Apollo 12 and SaU 169) provides strong evidence that these IMBs formed during a large impact into the PKT. Because of differences in the KREEP element concentrations and abundance patterns compared to typical Apollo 14 IMBs (Table 1, Fig. 2), we must consider that they might have formed in a different event than the one that formed the typical Apollo 14 breccias, i.e., presumably Imbrium. The most likely possibilities, on the basis of proximity to the PKT, include Serenitatis, Humorum, Nubium, and Insularum. Serenitatis, which is thought to have been sampled at the Apollo 17 site, produced IMBs that have KREEP-like abundance patterns, but lower concentrations, e.g., Th averaging 4–6 ppm and mostly less than 10 ppm (e.g., Jolliff et al., 1996). We do not think that impact melt produced in basin impacts must be uniform in composition, owing to the great size of such events and the likelihood of variable target deposits and composition (Haskin et al., 1998); however, the difference in composition, the distance of the Apollo 12 site from Serenitatis basin, and the fact that the high-Th IMBs are not found among Apollo 17, Apollo 15, and Apollo 14 samples argue against a Serenitatis origin.

The Humorum and Nubium basins lie just to the south of the Apollo 12 site and within the PKT, thus we consider that these events might have impacted Th-rich target rocks. Nubium is older (pre-Nectarian) than Humorum (Nectarian) (Wilhelms, 1987), thus we consider Humorum to be the more likely of the two basins to have deposited impact-melt in the central-PKT region where it could have been remobilized to the Apollo 12 regolith and the SaU 169 target regolith.

Even closer to the Apollo 12 site is the putative Insularum basin, the trace of which (if it exists) is very close to the Apollo 12 site (Fig. 7). Moreover, Copernicus crater impacted into a location near the center of the proposed Insularum basin. If that was the case, then we should not be surprised to find Insularum impact melt among the nonmare components of Apollo 12 regolith. Of course, Copernicus would also have ejected materials that lie above the Insularum impact melt sheet, including Fra Mauro-like deposits from Imbrium. Thus, if the Insularum basin exists, then it is likely

that large craters such as Copernicus, Reinhold, and Lansberg would have delivered components derived from its impact melt sheet or ejecta deposits to the Apollo 12 region. Reinhold and Lansberg may predate the basalts at the site, but local craters could excavate and mix their deposits into the present-day regolith. However, the existence of an Insularum basin, which was based originally on “circular patterns of terra islands in the western maria” (Wilhelms, 1987; Wilhelms and McCauley, 1971) is not supported by existence of a mascon or recent topographic analysis (Oberst et al., 2011, and personal communication). If an Insularum basin does exist, then it is highly degraded and thoroughly overprinted by Imbrium deposits, and certainly older than Serenitatis Basin. Next we consider the measured ages of the high-Th IMBs.

The Apollo 12 zircon $^{207}\text{Pb}/^{206}\text{Pb}$ age of 3914 ± 7 Ma reported here provides direct evidence of the age of the impact event that formed these melt breccias. The basis for this claim is that the zircon grains are demonstrably grown from the impact melt and are not inherited. This impact-melt crystallization age is identical, within error, to the zircon U–Pb age of 3920 ± 13 Ma reported here for the crystallization of the impact melt of SaU 169 and identical within uncertainty to the age of SaU 169 impact-melt crystallization of 3909 ± 13 Ma reported by Gnos et al. (2004). However, the age of these IMBs, taken as a group that dates a single event, is significantly older than the commonly quoted age of the Imbrium impact of 3850 ± 20 Ma, determined mainly by Ar–Ar and Rb–Sr on a variety of rocks, minerals, and breccias (Dalrymple and Ryder, 1996; Stöffler and Ryder, 2001; Stöffler et al., 2006; Wilhelms, 1987). One possibility is that the Th-rich IMBs were produced by one of the basins that is older than Imbrium, as discussed above, but not much older. Before we consider that possibility further, we look more closely at the Ar–Ar and Rb–Sr age determinations (see also Nyquist et al., 2011) and the possibility that the previously determined ages are actually consistent with the zircon ages determined herein and by Gnos et al.

A re-evaluation of the K–Ar decay constant proposed by Min et al. (2000) would increase the ^{40}Ar – ^{39}Ar age by about 1% and this increase would bring the Ar–Ar ages of KREEP-rich IMBs closer to the zircon age reported here. A revision to the age of the commonly used MMhb-1 monitor for Ar–Ar by 1.4–1.8% suggested by Renne et al. (1998) (see also Spell and McDougall, 2003, and Norman et al., 2010), would bring the Ar–Ar ages into the range of the zircon ages.

For lunar impact-melt rocks and breccia, there are fewer reported Rb–Sr ages than for ^{40}Ar – ^{39}Ar . For those ages calculated according to the Steiger and Jäger (1977) decay constant, a revision to the value of $1.402 \times 10^{-11} \text{ yr}^{-1}$ recommended by Minster et al. (1982) and Shih et al. (1985) or $1.394 \times 10^{-11} \text{ yr}^{-1}$ by Nebel et al. (2011) would bring ages of 3.84–3.85 Byr into agreement with our zircon age, within uncertainties. Begemann et al. (2001) discussed the ^{87}Rb decay constant and concluded that the value of Steiger and Jäger (1977) may be too high by 1 to 2%. Nyquist et al. (2011) reported an Rb–Sr age of an Apollo 16 mafic impact-melt rock 63545 that, along with an adjusted age for previously dated 67747 using the Shih et al. decay constant, yields a weighted average age of 3.90 ± 0.04 Ga and tentatively identified the age of this sample group with the Imbrium basin.

With regard to younger ages, one might also consider that the different ages register different intervals of the event, with the zircon age being a melt crystallization age and younger Rb–Sr and Ar–Ar ages being later cooling ages. However, this possibility would appear to be discounted by the U–Pb ages determined on apatite and zircon from Apollo 14 breccias reported by Nemchin et al. (2008). The U–Pb apatite age of 3926 ± 3 Ma was demonstrated to be a “reset age” formed by the complete Pb loss from older grains during the emplacement of the Fra Mauro Formation. Moreover, from a consideration of the Pb diffusion parameters of apatite and zircon, Nemchin et al. (2008) concluded that the Fra Mauro Formation was

deposited 3926 ± 3 Ma ago at a temperature between 1300°C and 1100°C but cooled sufficiently within a few years to close out the Rb–Sr and K–Ar systems.

In view of the simplicity of the interpretation of the zircon ages as crystallization ages and the known resistance of the zircon U–Pb system to later isotopic disturbance, we consider the present zircon U–Pb age of 3914 ± 7 Ma to be most simply interpreted as the age of the impact event, most likely Imbrium, with a caveat that the Imbrium target material was sufficiently heterogeneous to produce impact melt with the observed variability of KREEP-rich components as seen in materials from Apollo 12, 14, 15, and 16. Although an origin for the Apollo 12 high-Th IMBs as Insularum impact melt that was later excavated and delivered to the Apollo 12 site by one of the large post-Imbrium craters might be appealing, the lack of evidence for the existence of the Insularum basin or, at best, the advanced state of degradation makes it unlikely that this event would correspond to an age of only 3.91–3.92 Ga.

5.3. Implications for the cataclysm

Geochronological methods, including ^{40}Ar – ^{39}Ar , Rb–Sr, Sm–Nd, and U–Pb analyses, have recorded a widespread ~ 3.9 Ga age in Apollo and Luna samples. Many researchers (e.g., Tera et al., 1974) attributed this commonality to a large number of impact events in a short period of time (200 Ma or less), and this was referred to as the “lunar cataclysm.” ^{40}Ar – ^{39}Ar analyses in lunar meteorite breccias, which show a lack of impact melt ages older than 3.92 Ga, indicate that the cataclysm affected the entire Moon and likely the entire inner Solar System (Cohen et al., 2000). The age of the Imbrium impact and of the other more degraded basins is key to our understanding of the timing of the cataclysm, including the fact that there are many impact-melt samples with approximately this age. There are two possibilities for this correlation/situation, as follows: (1) All crystallization ages of KREEP-rich impact-melt breccias record the age of the Imbrium impact event, and the widely distributed ejecta of the Imbrium basin dominate the nearside chronology, as suggested by Baldwin (1974) and echoed by Haskin et al. (1998). (2) The Imbrium event was simply one of the last of many impacts of the lunar cataclysm that all occurred in a very short time interval. In this case, KREEP-bearing mafic impact-melt rocks and breccias would have been produced by more than one basin. The tight age distribution, however, would have to be reconciled with the apparently very different states of degradation of lunar impact basins and post-basin crater distributions superposed on basin ejecta deposits.

6. Conclusions

We have determined the ages of zircons in 5 different Apollo 12 high-Th impact-melt breccias. Nearly all of the zircons crystallized from the impact melt and, on the basis of the SHRIMP-II data, our preferred age for crystallization of the A12 high-Th IMB group is 3914 ± 7 Ma. Three inherited zircons are significantly older (> 4050 Ma). The Apollo 12 high-Th IMB group is, within analytical uncertainties, the same age as the SaU 169 IMB (3916 ± 15 Ma as reported here). These two different samples of Th-rich IMBs are geochemically and petrologically very similar, and we consider them to be part of the same IMB group.

If the high-Th IMB group at the Apollo 12 site ultimately had a basin origin, then it is most likely to be derived from the Imbrium event. However, we do not interpret this material as primary Imbrium ejecta, but rather as Imbrium ejecta that was remobilized by one or more later, medium-sized, post-basin impacts into an Imbrium ejecta deposit, most likely Copernicus, but possibly also Reinhold or Lansberg. The later impact(s) that delivered the IMBs to the Apollo 12 site (and the SaU 169 source region) did not reset the zircon ages.

The age of the Apollo 12 high-Th IMB group is significantly (with respect to measurement uncertainty) older than the commonly quoted age of Imbrium, 3850–3865 Ma, but this age determination has been based mainly on Ar–Ar dating of Apollo IMBs, with some determinations by Rb–Sr, and these ages should be revised as discussed above. Ages so revised appear to be consistent with the zircon ages determined by us and by Gnos et al. for the SaU 169 impact melt phase. We conclude that the age of the Apollo 12 high-Th IMBs most likely represents the age of the Imbrium event and specifically that the age of these zircons reflects the age of the Imbrium impact melt crystallization, as Gnos et al. (2004) also concluded for SaU 169.

Acknowledgments

We thank NASA for support through grant NNG04GG10G (RLK). We also acknowledge the Ministry of Science and Technology of China for support through grant 2009IM030800. We are grateful for support from the McDonnell Center for the Space Sciences, which enabled BJ and RAZ to visit the SHRIMP-II lab in Beijing and provided seed funds for this collaboration. We thank Beda Hoffman and the Natural History Museum of Bern for providing the SaU 169 samples for analysis. We thank R. T. Pidgeon for assistance during preparation of the manuscript. The manuscript was greatly improved by comments from reviews by Marc Norman and an anonymous reviewer.

Appendix A. Supplementary data

Supplementary data to this article can be found online at [doi:10.1016/j.epsl.2011.12.014](https://doi.org/10.1016/j.epsl.2011.12.014).

References

- Baldwin, R.B., 1974. Was there a “terminal lunar cataclysm” 3.9–4.0 $\times 10^9$ years ago? *Icarus* 23, 157–166.
- Begemann, F., Ludwig, K.R., Lugmair, G.W., Min, K., Nyquist, L.E., Patchett, P.J., Renne, P.R., Shih, C.-Y., Villa, I.M., Walker, R.J., 2001. Call for an improved set of decay constants for geochronological use. *Geochim. Cosmochim. Acta* 65, 111–121.
- Cohen, B.A., Swindle, T.D., Kring, D.A., 2000. Support for the lunar cataclysm hypothesis from lunar meteorite impact melt ages. *Science* 290, 1754–1756.
- Dalrymple, G.B., Ryder, G., 1996. Argon-40/Argon-39 age spectra of Apollo 17 highlands breccia samples by laser step heating and the age of the Serenitatis basin. *J. Geophys. Res.* 101, 26,069–26,084.
- Elphic, R.C., Lawrence, D.J., Feldman, W.C., Barraclough, B.L., Maurice, S., Binder, A.B., Lucey, P.G., 2000. Lunar rare earth element distribution and ramifications for FeO and TiO₂: Lunar Prospector neutron spectrometer observations. *J. Geophys. Res.* 105, 20,333–20,345.
- Feldman, W.C., Barraclough, B.L., Fuller, K.R., Lawrence, D.J., Maurice, S., Miller, M.C., Prettyman, T.H., Binder, A.B., 1999. The Lunar Prospector gamma-ray and neutron spectrometers. *Nucl. Instrum. Methods Phys. Res.* 422A, 562–566.
- Gnos, E., Hofmann, B.A., A., A.-K., Lorenzetti, S., Eugster, O., Whitehouse, M.J., Villa, I.M., Jull, A.J.T., Eikenberg, J., Spettel, B., Krähenbühl, U., Franchi, I.A., Greenwood, R.C., 2004. Pinpointing the source of a lunar meteorite: implications for the evolution of the Moon. *Science* 305, 657–659.
- Haskin, L.A., Korotev, R.L., Rockow, K.M., Jolliff, B.L., 1998. The case for an Imbrium origin of the Apollo Th-rich impact-melt breccias. *Meteorit. Planet. Sci.* 33, 959–975.
- Jolliff, B.L., 1998. Large-scale separation of K-fraction and REEP-fraction in the source regions of Apollo impact-melt breccias, and a revised estimate of the KREEP composition. *Int. Geol. Rev.* 40, 916–935.
- Jolliff, B.L., Korotev, R.L., Haskin, L.A., 1991. Geochemistry of 2–4 mm particles from Apollo 14 soil (14161) and implications regarding igneous components and soil-forming processes. *Proceedings of the Lunar and Planetary Science Conference*, 21, pp. 193–219.
- Jolliff, B.L., Rockow, K.M., Korotev, R.L., Haskin, L.A., 1996. Lithologic distribution and geologic history of the Apollo 17 site: The record in soils and small rock particles from the highland massifs. *Meteor. Planet. Sci.* 31, 116–145.
- Korotev, R.L., 1991. Geochemical stratigraphy of two regolith cores from the central highlands of the Moon. *Proc. Lunar Planet. Sci.* 21, 229–289.
- Korotev, R.L., 2000. The great lunar hot spot and the composition and origin of the Apollo mafic (“LKF”) impact-melt breccias. *J. Geophys. Res.* 105, 4317–4345.
- Korotev, R.L., Jolliff, B.L., Zeigler, R.A., Seddio, S.M., Haskin, L.A., 2011. Apollo 12 revisited. *Geochim. Cosmochim. Acta.* 75, 1540–1573.
- Lawrence, D.J., Feldman, W.C., Barraclough, B.L., Binder, A.B., Elphic, R.C., Maurice, S., Thomsen, D.R., 1998. Global elemental maps of the Moon: The Lunar Prospector gamma-ray spectrometer. *Science* 281, 1484–1489.

- Lawrence, D.J., Feldman, W.C., Barraclough, B.L., Binder, A.B., Elphic, R.C., Maurice, S., Miller, M.C., Prettyman, T.H., 2000. Thorium abundances on the lunar surface. *J. Geophys. Res.* 105, 20,307–20,331.
- Meyer, C., Williams, I.S., Compston, W., 1996. Uranium-lead ages for lunar zircons: evidence for a prolonged period of granophyre formation from 4.32 to 3.88 Ga. *Meteorit. Planet. Sci.* 31, 370–387.
- Min, K., Mundil, R., Renne, P.R., Ludwig, K.R., 2000. A test for systematic errors in $^{40}\text{Ar}/^{39}\text{Ar}$ geochronology through comparison with U–Pb analysis of a 1.1 Ga rhyolite. *Geochim. Cosmochim. Acta.* 64, 73–98.
- Minster, J.-F., Birck, J.-L., Allègre, C.J., 1982. Absolute age of formation of chondrites studied by the ^{87}Rb – ^{87}Sr method. *Nature* 300, 414–419.
- Nebel, O., Scherer, E., Mezger, K.E., 2011. Evaluation of the ^{87}Rb decay constant by age comparison against the U–Pb system. *Earth Planet. Sci. Lett.* 301, 1–8.
- Nemchin, A.A., Pidgeon, R.T., Whitehouse, M.J., Vaughan, J.P., Meyer, C., 2008. SIMS U–Pb study of zircon from Apollo 14 and 17 breccias: implications for the evolution of lunar KREEP. *Geochim. Cosmochim. Acta.* 72, 668–689.
- Nemchin, A.A., Pidgeon, R.T., Healy, D., Grange, M.L., Whitehouse, M.J., Vaughan, J., 2009. The comparative behavior of apatite-zircon U–Pb systems in Apollo 14 breccias: implications for the thermal history of the Fra Mauro Formation. *Meteorit. Planet. Sci.* 44, 1717–1734.
- Norman, M.D., Duncan, R.A., Huard, J.J., 2010. Imbrium provenance for the Apollo 16 Descartes terrain: argon ages and geochemistry of lunar breccias 67016 and 67455. *Geochim. Cosmochim. Acta.* 74, 763–783.
- Nyquist, L.E., Shih, C.-Y., Reese, Y.D., 2011. Dating melt rock 63545 by Rb–Sr and Sm–Nd: age of Imbrium; SPA Dress Rehearsal. *Lunar Planet. Sci.* 42 #1868.
- Oberst, J., Unbekannt, H., Scholten, F., Haase, I., Hiesinger, H., Robinson, M., 2011. A search for degraded lunar basins using the LROC-WAC Digital Terrain Model (GLD100). 42nd Lunar and Planetary Science Conference, Abstract #1992.
- Reedy, R.C., 1978. Planetary gamma-ray spectroscopy. *Proc. Lunar Planet. Sci. Conf.* 9th, pp. 2961–2984.
- Renne, P.R., Swisher, C.C., Deino, A.L., Karner, D.B., Owens, T.L., DePaolo, D.J., 1998. Intercalibration of standards, absolute ages and uncertainties in $^{40}\text{Ar}/^{39}\text{Ar}$ dating. *Chem. Geol.* 145, 117–152.
- Robinson, M.S., Brylow, S.M., Tschimmel, M., Humm, D., Lawrence, S.J., Thomas, P.C., Denevi, B.W., Bowman-Cisneros, E., Zerr, J., Ravine, M.A., Caplinger, M.A., Ghaemi, F.T., Schaffner, J.A., Malin, M.C., Mahanti, P., Bartels, A., Anderson, J., Tran, T.N., Eliason, E.M., McEwen, A.S., Turtle, E., Jolliff, B.L., Hiesinger, H., 2010. Lunar Reconnaissance Orbiter Camera (LROC) Instrument Overview. *Space Science Reviews* 150, 81–124.
- Russell, S.S., Zipfel, J., Folco, L., Jones, R., Grady, M.M., McCoy, T., Grossman, J.N., 2003. The Meteoritical Bulletin, No. 87, 2003 July. *Meteorit. Planet. Sci.* 38, A194.
- Ryder, G., Spudis, P., 1987. Chemical composition and origin of Apollo 15 impact melts. *J. Geophys. Res.* 92, E432–E446.
- Shih, C.-Y., Nyquist, L.E., Bogard, D.D., Wooden, J.L., Bansal, B.M., Wiesmann, H., 1985. Chronology and petrogenesis of a 1.8 g lunar granitic clast: 14321,1062. *Geochim. Cosmochim. Acta* 49, 411–426.
- Spell, T.L., McDougall, I., 2003. Characterization and calibration of $^{40}\text{Ar}/^{39}\text{Ar}$ dating standards. *Chem. Geol.* 198, 189–211.
- Stacey, J.S., Kramers, J.D., 1975. Approximation of terrestrial lead isotope evolution by a two-stage model. *Earth Planet. Sci. Lett.* 28, 207–221.
- Steiger, R.H., Jäger, E., 1977. Subcommittee on geochronology: convention on the use of decay constants in geo- and cosmochronology. *Earth Planet. Sci. Lett.* 36, 359–362.
- Stern, R.A., 2001. A new isotopic and trace-element standard for the ion microprobe: preliminary thermal ionization mass spectrometry (TIMS) U–Pb and electron-microprobe data; radiogenic age and isotopic studies: Report 14, Geological Survey of Canada, Current Research 2001-F1, 11 pp.
- Stöfler, D., Ryder, G., 2001. Stratigraphy and isotope ages of lunar geologic units: chronological standard for the Inner Solar System. *Space Sci. Rev.* 96, 9–54.
- Stöfler, D., Ryder, G., Ivanov, B.A., Artemieva, N.A., Cintala, M.J., Grieve, R.A.F., 2006. Cratering history and lunar chronology. In: Jolliff, B.L., Wieczorek, M.A., Shearer, C.K., Neal, C.R. (Eds.), *New Views of the Moon, Reviews in Mineralogy and Geochemistry*, Vol. 60. Mineralogical Society of America and Geochemical Society, pp. 519–596.
- Tera, F., Papanastassiou, D.A., Wasserburg, G.J., 1974. Isotopic evidence for a terminal lunar cataclysm. *Earth Planet. Sci. Lett.* 22, 1–21.
- Trail, D., Mojzsis, S.J., Harrison, T.M., 2007. Thermal events documented in Hadean zircons by ion microprobe depth profiles. *Geochim. Cosmochim. Acta.* 71, 4044–4065.
- Warner, J., 1971. Apollo 12 lunar sample information. NASA Tech. Report. . 377 pp.
- Warren, P.H., 1989. KREEP: major-element diversity, trace-element uniformity (almost). In: Taylor, G.J., Warren, P.H. (Eds.), *Workshop on Moon in Transition: Apollo 14, KREEP, and Evolved Lunar Rocks* LPI Tech. Report. 89-03, Lunar and Planetary Institute, Houston, pp. 149–153.
- Wilhelms, D.E., 1987. The geologic history of the moon. *U.S. Geol. Surv. Prof. Pap.* 1348, 302 pp.
- Wilhelms, D.E., McCauley, J.F., 1971. Geologic map of the near side of the moon, miscellaneous geologic investigations. USGS Map I-703, U.S. Geological Survey, Washington, D.C. .
- Williams, I.S., 1998. U–Th–Pb geochronology by ion microprobe. In: McKibben, M.A., Shanks III, W.C., Ridley, W.I. (Eds.), *Applications of microanalytical techniques to understanding mineralizing processes*: *Rev. Econ. Geol.* , pp. 1–35.
- Zeigler, R.A., Korotev, R.L., Jolliff, B.L., Haskin, L.A., 2005. Petrology and geochemistry of the LaPaz icefield basaltic lunar meteorite and source-crater pairing with Northwest Africa 032. *Meteorit. Planet. Sci.* 40, 1073–1102.
- Zeigler, R.A., Korotev, R.L., Jolliff, B.L., 2006. Geochemistry and petrography of high-Th, mafic impact-melt breccia from Apollo 12 and Sayh Al Uhaymir 169. *Proc. Lunar Planet. Sci. Conf.* XXXVII, Abstract no. 2366.